Available online at www.sciencedirect.com

SciVerse ScienceDirect

journal homepage: www.elsevier.com/locate/he

Ethanol and glycerin processor systems coupled to solid oxide fuel cells (SOFCs). Optimal operation and heat exchangers network synthesis

*Diego G. Oliva, Javier A. Francesconi, Miguel C. Mussati, Pio A. Aguirre**

INGAR, Instituto de Desarrollo y Diseño (CONICET-UTN), Avellaneda 3657, S3002GJC Santa Fe, Argentina

ARTICLE INFO

Article history:
Received 29 November 2012
Received in revised form
7 March 2013
Accepted 13 March 2013
Available online 24 April 2013

Keywords:
Ethanol processor
Glycerin processor
Solid oxide fuel cell
Optimal HEN synthesis
Optimal operation

ABSTRACT

This paper is aimed at presenting a methodology for the simultaneous synthesis of solid oxide fuel cell (SOFC) based systems and their associated heat exchangers network (HEN). The optimization model is formulated as a mixed integer nonlinear mathematical programming (MINLP) problem. The optimization goal is to maximize the overall net efficiency of the integrated system.

Ethanol and glycerin are studied as fuels fed to the SOFC system as they constitute two renewable and sustainable sources of energy.

As main results, net global efficiency values of 69.35% and 66.97% were computed for ethanol and glycerin, respectively. For both cases, the computed optimal operation pressure, the SOFC operation temperature and the fed water/fuel molar ratio values were 2 atm, 1073 K and 3, respectively.

1. Introduction

The solid oxide fuel cells (SOFCs) are currently designed based on two main geometrical configuration types: planar or tubular. A detailed literature review on SOFCs modeling has been performed by Janardhanan and Deutschmann [1]. Ni et al. [2] have conducted parametric studies on SOFCs fed with bio-gas as fuel, evaluating the relation between the electrode porosity and performance (overpotentials) at different temperature and pressure levels. Yakabe et al. [3] have developed a detailed mathematical model for predicting the electric current, potential, temperature and concentration profiles inside a SOFC. Achenbach [4] has simulated planar SOFCs type fed with methane resorting to a tri-dimensional mathematical model, considering a recirculation stream of the out-coming gas from the anode, and both co-current and counter-current fuel flow patterns inside the cell. The author reported the predicted current density, gas concentration and temperature profiles inside the cell. Bhattacharyya et al. [5] have developed a dynamic model for a tubular SOFC type based on experimental data obtained from an industrial unit operating at different scenarios. Mollayi Barzi et al. [6] derived a dynamic two-dimensional model for tubular SOFC type, considering mass, momentum and energy balances. The model accounts for cell overpotentials by mimicking an equivalent electrical circuit. Cimenti and Hill [7] have performed a thermodynamic analysis of SOFCs fed directly with different vaporized mixtures of water/methane and water/

* *Corresponding author*. Tel.: +54 342 453 4451; fax: +54 342 455 3439.
E-mail addresses: doliva@santafe-conicet.gov.ar (D.G. Oliva), javierf@santafe-conicet.gov.ar (J.A. Francesconi), mmussati@santafe-conicet.gov.ar (M.C. Mussati), paguir@santafe-conicet.gov.ar (P.A. Aguirre).
0360-3199/$ – see front matter
http://dx.doi.org/10.1016/j.ijhydene.2013.03.073

ethanol for determining the carbon formation region for each case. Bove et al. [8] developed a simplified model for SOFCs to reduce its mathematical complexity and facilitate the behavioral analysis of a SOFC system coupled to a power cycle consisting on an expander turbine; i.e. pumps, reformer, SOFC unit, compressor and turbine. Burbank et al. [9] developed configurations for operating at stable temperature the power cycle turbine coupled to the SOFC unit using turbines with variable injectors, fueling natural gas. Cocco and Tola [10] simulated two SOFC-power cycle configurations in ASPEN environment; in one case the cell was fed with the out-coming stream from the fuel reforming unit, while in the other one the fuel was fed directly without prior reforming. The work was conducted with different fuels fixing the reactors temperature. The results showed relative advantages and disadvantages of each configuration, as well as the more suitable fuel for each one. Costamagna et al. [11] proposed a SOFC model considering technological limitations in the process units involved in the coupled SOFC-turbine process. Petruzzi et al. [12] developed a thermo-electrochemical model of a SOFC for evaluating start-up times, stack configurations and insulation required for safe operation as auxiliary power units in vehicles. Yi et al. [13] investigated a coupled SOFC-power cycle system fueled with humidified methane to analyze the influence of the system pressure, the fed methane-to-water ratio, and the air excess on the system efficiency.

Arteaga-Pérez et al. [14] have simulated an ethanol processing system coupled to a SOFC. The authors firstly analyzed the fuel utilization factor, the water-to-ethanol molar ratio, and the reformer temperature. Afterward, they addressed the heat exchangers network (HEN) synthesis resorting to the "pinch" methodology. This approach is of the "onion skin" diagram type: firstly, the process units and streams are determined and, secondly, the operating conditions are fixed to address the HEN synthesis problem. Palazzi et al. [15] developed a thermo-economic model of the process, based on which they performed a sequential optimization by computing first the process operation variables, and synthesizing then the HEN to obtain the system efficiency, process units size and costs. They formulated a multi-objective optimization problem, and presented the obtained results in a Pareto chart, where optimal efficiency values were plotted against economic ones.

Due to the high SOFC operation temperature level, Autissier et al. [16] carried out an economic analysis for a number of feasible cell designs, determining cost-to-efficiency ratios for each case, using natural gas as fuel. Santin et al. [17] performed an economic analysis of tubular and planar SOFCs coupled to an expander turbine, but fueled with either methanol or kerosene.

In this context, it can be noted that there has been published several papers dealing first with the analysis and optimization of SOFC-based systems, and then, with the associated HEN synthesis. However, to the authors' knowledge, there are no papers addressing *simultaneously* the optimization of SOFC-based processes with the associated HEN.

This paper is thus aimed at presenting a methodology for the simultaneous synthesis of SOFC-based systems and their associated heat exchangers networks. Then, the traditional resolution approach based on the *onion skin diagram* and *hierarchy of analysis* can be avoided.

From a methodological point of view, it should be noted that if other processes are considered, the modeler has to formulate or adapt the associated HENs to the corresponding process model in order to solve the mass and energy balances simultaneously; i.e. the proposed methodology is not intended to be a benchmark in which the modeler has only to substitute a given process model by other model to obtain the optimal process-HEN configuration.

This paper is organized as follows. The investigated process is briefly described in Section 2. The mathematical model representing the SOFC system is presented in Section 3. The optimization problem is stated and formulated in Section 4. The proposed resolution methodology and numerical aspects are presented in Section 5. Results obtained using either ethanol or glycerin as fuels are discussed in Section 6. Finally, conclusions are drawn in Section 7.

2. Process description

The investigated system is a process consisting on a fuel reformer, SOFC unit, combustor, expander turbine, fuel pumps, air compressors, and heat exchangers. Fig. 1 shows a basic layout of the considered process without energy integration. Fuels fed to the SOFC system are either ethanol or glycerin.

3. Process model

3.1. *Concept of stream state*

Prior to model derivation of the investigated SOFC system, the conceptual modeling framework is briefly presented.

Fig. 2 schematizes a part of a flow sheet of a given process consisting of two reactors in-series and their process streams (not integrated energetically), whose energy requirements are satisfied by a heat exchanger. $C_{r,j}$ represents a stream "r" at state "j", what hereafter is referred as "stream-state" for brevity. Each state has an associated vector whose components are the values of the enthalpy, composition and pressure variables (called "main variables") and the values of the temperature and component partial pressure variables (called "dependent variables"), which are dependent from the main variables. $Q_{p,m,n}$ represents the heat exchanged by stream "p" from initial state "m" to another state "n". In Fig. 2, the dependent variables are indicated by "*" while the main ones by "-". It is assumed gas ideal behavior for enthalpy value estimation in the investigated operation pressure range. However, the pressure is taken into account for calculating the bubble point.

The presence of process unit "Reactor 1" determines the existence of two streams (streams "1" and "2") as the chemical composition changes inside it. Analogously, the presence of process unit "Reactor 2" determines the existence of stream "3" as the chemical composition of the inlet stream "2" changes when passing through it. The existence of a heat exchange unit (without reaction and mass transfer)

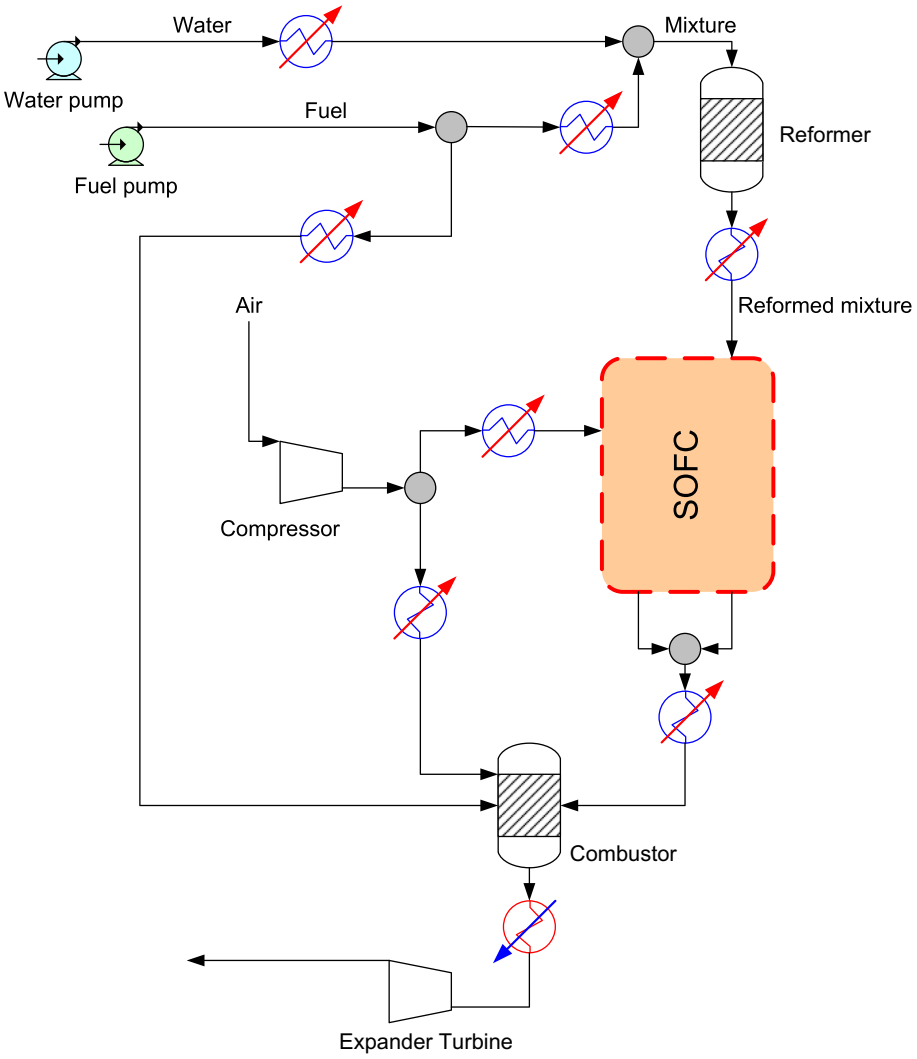

Fig. 1 – Simplified diagram of energy production system through a SOFC that uses liquid fuel "SOFC system".

determines that stream "2" has two possible states: the inlet exchanger state and the outlet exchanger state. The particular process here investigated is now schematized in Fig. 3 using the concept of system states. B1 and B2 are the water and fuel pumps, respectively; C1 and C2 are air compressors in-series prior to combustor and SOFC. T1 is an expander turbine powered by the exhaust gases from the combustor.

Pumps and compressors raise the pressure of liquids and air, respectively, to the system operation pressure. The expander turbine ejects gases at atmospheric pressure.

Process streams and their states are detailed in Table 1 according to Fig. 3. Table 2 lists the heat requirements involved in the change of the streams state. In Fig. 3, heating and cooling requirements in a heat exchanger are indicated by arrows up and down, respectively.

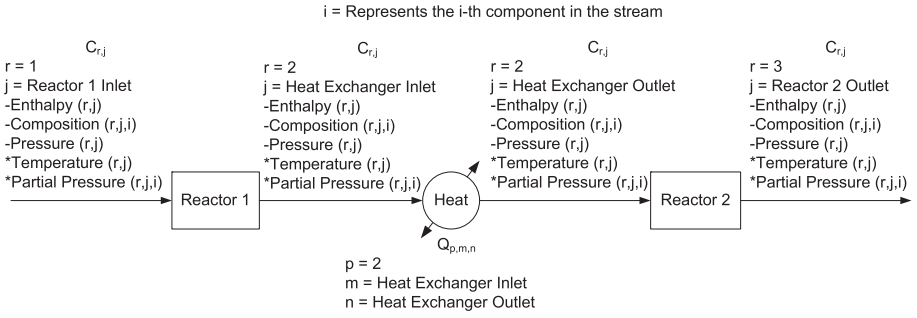

Fig. 2 – Diagram of the conceptual modeling. Definition of streams as system states.

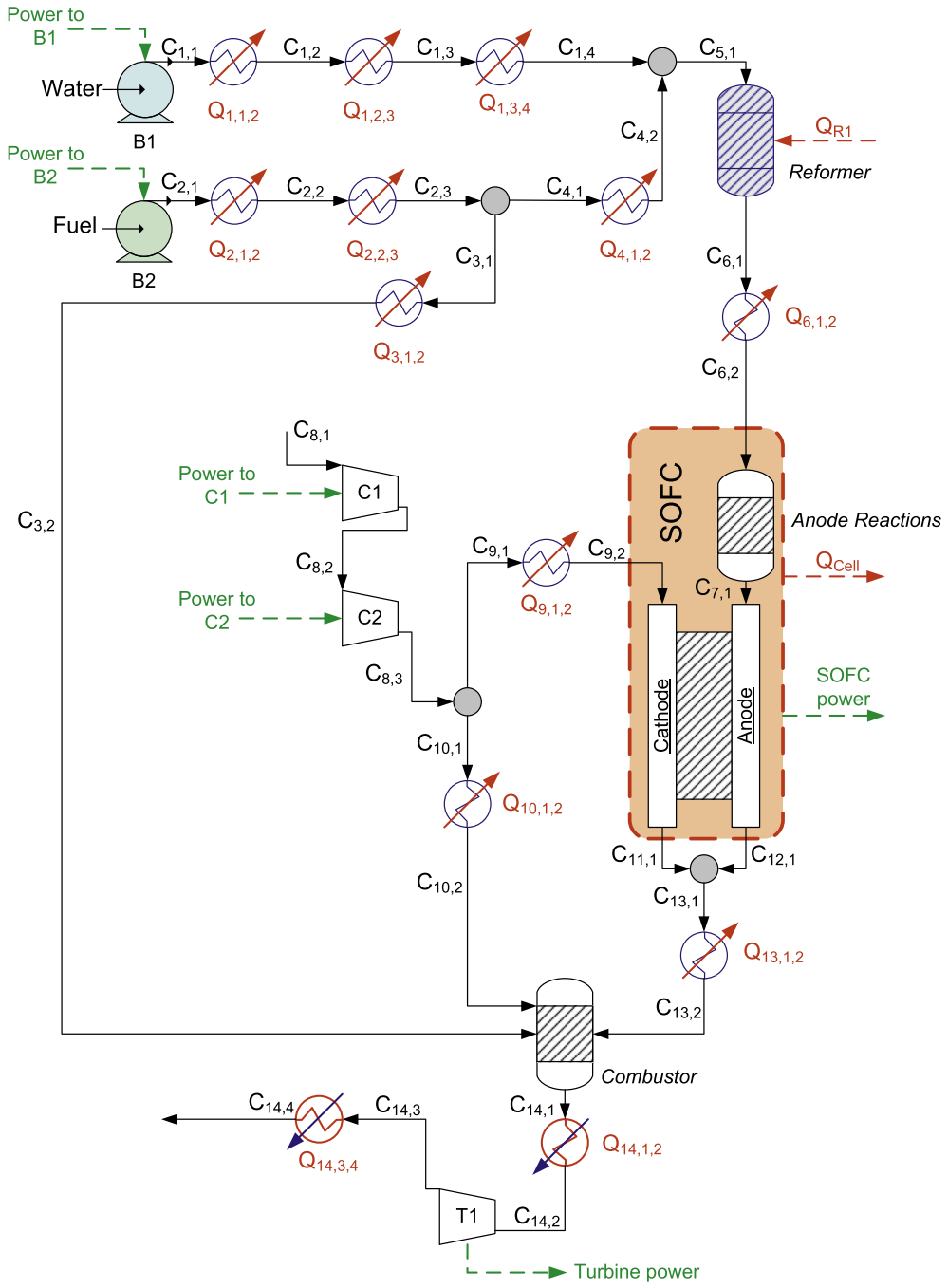

Fig. 3 – Power generation system by a SOFC using a liquid fuel. Scheme of the process stream-states.

3.2. *Estimation of stream's variable values at states*

The expressions for computing the streams enthalpy value at each state depend on the stream aggregation state.

3.2.1. *Pure liquid enthalpy*

The saturation temperature Ts of the component l is implicitly calculated by the Antoine equation as follows:

$$\mathrm{Log}(P_{\mathrm{total}}) = \frac{\alpha_{A,l} + \alpha_{B,l}}{\alpha_{C,l} + \mathrm{Ts}_l} + \alpha_{D,l} \cdot \mathrm{Log}(\mathrm{Ts}_l) + \alpha_{E,l} \cdot (\mathrm{Ts}_l)^{\alpha_{F,l}} \quad (1)$$

where P_{total} is the total pressure; α are the Antoine coefficients. The pure liquid enthalpy Hl_l is calculated by the following expression:

$$\mathrm{Hl}_l = \mathrm{Hv}_l - \Delta H_{\mathrm{Vap}_l} - \Delta H_{\mathrm{Liq}_l} \quad (2)$$

where Hv_l is the vapor enthalpy of compound l at the saturation temperature Ts; $\Delta H_{\mathrm{Vap}_l}$ is the latent vaporization heat, and $\Delta H_{\mathrm{Liq}_l}$ is the liquid sensible heat to raise the temperature of compound l from T_l to its saturation temperature Ts. Hv_l, $\Delta H_{\mathrm{Vap}_l}$ and $\Delta H_{\mathrm{Liq}_l}$ are estimated using the correlations (3)–(5), respectively:

Table 1 – Process streams and state.

Stream	Description
$C_{1,1}$	Pure water fed to the system
$C_{1,2}$	Water at boiling point
$C_{1,3}$	Steam at boiling point
$C_{1,4}$	Superheated steam
$C_{2,1}$	Pure fuel fed to the system
$C_{2,2}$	Fuel at boiling point
$C_{2,3}$	Fuel vapor at boiling point
$C_{3,1}$	Fuel vapor at saturation temperature fed to combustor
$C_{3,2}$	Fuel vapor fed to combustor
$C_{4,1}$	Fuel vapor at saturation temperature fed to reformer
$C_{4,2}$	Fuel vapor fed to reformer
$C_{5,1}$	Water/fuel mixture fed to reformer
$C_{6,1}$	Reformed gas output
$C_{6,2}$	Reformed gas output
$C_{7,1}$	Reformed gases to anode
$C_{8,1}$	Air fed to the system
$C_{8,2}$	Compressor C1, air output
$C_{8,3}$	Compressor C2, air output
$C_{9,1}$	Air fed to SOFC cathode
$C_{9,2}$	Air fed to SOFC cathode
$C_{10,1}$	Air fed to combustor
$C_{10,2}$	Air fed to combustor
$C_{11,1}$	Output gases from cathode
$C_{12,1}$	Output gases from anode
$C_{13,1}$	SOFC output gases fed to combustor
$C_{13,3}$	SOFC output gases fed to combustor
$C_{14,1}$	Output gases from combustor
$C_{14,2}$	Output gases from combustor
$C_{14,3}$	Output gases from T1 turbine expander
$C_{14,4}$	Output gases from T1 turbine expander

$$\mathrm{Hv_l}\cdot 1000 = \Delta H_{\mathrm{form,l}} + \beta_{\mathrm{A,l}}\cdot\left(\mathrm{Ts_l} - T_{\mathrm{ref}}\right) + \frac{\beta_{\mathrm{B,l}}\cdot\left(\mathrm{Ts_l^2} - \mathrm{T_{ref}^2}\right)}{2} + \frac{\beta_{\mathrm{C,l}}\cdot\left(\mathrm{Ts_l^3} - \mathrm{T_{ref}^3}\right)}{3} + \frac{\beta_{\mathrm{D,l}}\cdot\left(\mathrm{Ts_l^4} - \mathrm{T_{ref}^4}\right)}{4} + \frac{\beta_{\mathrm{E,l}}\cdot\left(\mathrm{Ts_l^5} - \mathrm{T_{ref}^5}\right)}{5} \quad (3)$$

$$Log\left(\Delta H_{\mathrm{Vap_l}}\cdot 1000\right) = Log(\delta_{\mathrm{A,l}}) + Log\left(1 - \frac{T_{S_l}}{T_{C_l}}\right)\cdot\delta_{\mathrm{B,l}} + \delta_{\mathrm{C,l}}\cdot\frac{T_{S_l}}{T_{C_l}} + \delta_{\mathrm{D,l}}\cdot\left(\frac{T_{S_l}}{T_{C_l}}\right)^2 + \delta_{\mathrm{E,l}}\cdot\left(\frac{T_{S_l}}{T_{C_l}}\right)^3 \quad (4)$$

$$\Delta H_{\mathrm{Liq_l}}\cdot 1000 = \phi_{\mathrm{A,l}}\cdot\left(\mathrm{Ts_l} - \mathrm{T_l}\right) + \frac{\phi_{\mathrm{B,l}}\cdot\left(\mathrm{Ts_l^2} - \mathrm{T_l^2}\right)}{2} + \frac{\phi_{\mathrm{C,l}}\cdot\left(\mathrm{Ts_l^3} - \mathrm{T_l^3}\right)}{3} + \frac{\phi_{\mathrm{D,l}}\cdot\left(\mathrm{Ts_l^4} - \mathrm{T_l^4}\right)}{4} + \frac{\phi_{\mathrm{E,l}}\cdot\left(\mathrm{Ts_l^5} - \mathrm{T_l^5}\right)}{5} \quad (5)$$

where $\beta_{D,l}$, $\delta_{D,l}$ and $\phi_{D,l}$ are coefficients and subscript l refers to a component. $\Delta H_{form,l}$ is the formation enthalpy of the pure component l at the reference temperature T_{ref}.

3.2.2. *Gas mixture enthalpy*

Most gaseous process streams are gas mixtures, except for vaporized fuel and water steam streams.

The enthalpy of a gas mixture stream is computed as the weighted average of the enthalpy of each pure component of the mixture.

Table 2 – Heat requirement of streams.

Name	Description
$Q_{1\text{-}1\text{-}2}$	Heating of liquid water
$Q_{1\text{-}2\text{-}3}$	Phase change heat energy
$Q_{1\text{-}3\text{-}4}$	Heating of steam
$Q_{2\text{-}1\text{-}2}$	Heating of liquid fuel
$Q_{2\text{-}2\text{-}3}$	Fuel phase change heat energy
$Q_{3\text{-}1\text{-}2}$	Heating of vaporized fuel
$Q_{4\text{-}1\text{-}2}$	Heating of vaporized fuel
$Q_{6\text{-}1\text{-}2}$	Heating of reformed gases
$Q_{9\text{-}1\text{-}2}$	Heating of air supplied to SOFC
$Q_{10\text{-}1\text{-}2}$	Heating of air supplied to combustor
$Q_{13\text{-}1\text{-}2}$	Heating of gases from SOFC
$Q_{14\text{-}1\text{-}2}$	Heating of output gases from combustor supplied to turbine
$Q_{14\text{-}3\text{-}4}$	Heating of turbine output gases
Q_{Cell}	Heat from SOFC
Q_{R1}	Heat to reforming reactor

The enthalpy of the component i in the gas stream s ($\mathrm{Hv_{i,s}}$) is computed using the formation enthalpy of the pure compound i at the reference temperature T_{ref} ($\Delta H_{form,i}$) by the following correlation:

$$\mathrm{Hv_{i,s}}\cdot 1000 = \Delta H_{\mathrm{form,i}} + \beta_{\mathrm{A,i}}\cdot\left(T_s - T_{\mathrm{ref}}\right) + \frac{\beta_{\mathrm{B,i}}\cdot\left(\mathrm{T_s^2} - \mathrm{T_{ref}^2}\right)}{2} + \frac{\beta_{\mathrm{C,i}}\cdot\left(\mathrm{T_s^3} - \mathrm{T_{ref}^3}\right)}{3} + \frac{\beta_{\mathrm{D,i}}\cdot\left(\mathrm{T_s^4} - \mathrm{T_{ref}^4}\right)}{4} + \frac{\beta_{\mathrm{E,i}}\cdot\left(\mathrm{T_s^5} - \mathrm{T_{ref}^5}\right)}{5} \quad (6)$$

The average enthalpy of stream s ($\mathrm{Hvm_s}$) is computed by:

$$\mathrm{Hvm_s} = \frac{\sum_i F_{i,s}\cdot \mathrm{Hv_{i,s}}}{3600} \quad (7)$$

where $F_{i,s}$ is the molar flux of compound i in stream s.

3.3. *Partial pressure of a component in a stream*

The partial pressure P_i of a component i is computed as:

$$P_i = P_{\mathrm{total}}\cdot y_i \quad (8)$$

where P_{total} is the total pressure of the stream, and y_i is the molar fraction of compound i in the mixture.

3.4. *Reforming reactions*

The reforming reactions taking place in the reformer depend on the used fuel. In this paper, the schemes of reactions for ethanol and glycerin reforming processes proposed by Francesconi et al. [18] and Hirai et al. [19], respectively, are adopted. The

reforming reactor is modeled as an isothermal equilibrium reactor.

3.5. *Fuel cell model*

The SOFC model derivation is based on modeling hypotheses assumed in previous works [18,20].

The SOFC unit is fed with the gas mixture resulting from the fuel steam reforming. Independently of the used fuel, the compounds present in the reformed gas mixture fed to the anode are H_2, H_2O, CO, CO_2 and CH_4, but their relative amounts depend on it, as analyzed later. The cathode is fed with an air stream (N_2 and O_2).

The anode and cathode are considered separately. In order to represent the simultaneous electro-oxidation of H_2 and CO, the SOFC is modeled as two in-parallel fuel cells. It is assumed that the H_2 electro-oxidation takes places at the anode of the first cell (Cell1):

$$H_2 + O^{2-} \rightarrow H_2O + 2e^-$$

and the CO electro-oxidation at the anode of the second cell (Cell2):

$$CO + O^{2-} \rightarrow CO_2 + 2e^-$$

The following reduction occurs at the cathode of both cells:

$$\frac{1}{2}O_2 + 2e^- \rightarrow O^{2-}$$

In addition, the following reactions in equilibrium are considered at the SOFC operation temperature (T_{SOFC}):

- CH_4 reforming:

$$CH_4 + H_2O \overset{Keq_{CH_4}}{\rightleftharpoons} CO + 3H_2$$

$$\log\left(Keq_{CH_4}\right) = -20.5524 - 22920\cdot\frac{6}{T_{SOFC}} + 7.19465\cdot log(T_{SOFC}) - 2.94944\cdot10^{-3}\cdot T_{SOFC} \quad (9)$$

- Water gas shift reaction (WGS):

$$CO + H_2O \overset{Keq_{WGS}}{\rightleftarrows} CO_2 + H_2$$

$$\log(Keq_{WGS}) = -12.1076 + 5318\cdot\frac{69}{T_{SOFC}} + 1.01205\cdot log(T_{SOFC}) + 1.14367\cdot10^{-4}\cdot T_{SOFC} \quad (10)$$

where Keq_{CH_4} and Keq_{WGS} are the equilibrium constants in Eqs. (9) and (10), respectively.

The normal reversible potential (E^0) (at normal conditions of pressure and temperature) of an electrochemical reaction is defined as:

$$E^0 = \frac{-\Delta G^0_{Rx}}{ne\cdot Fa} \quad (11)$$

where ne is the number of electrons involved in the reaction, Fa is the Faraday constant (96,487 C mol^{-1}), and ΔG^0_{Rx} is the change in Gibbs free energy for the reaction Rx (J mol^{-1}) at normal conditions of pressure and temperature, which is defined as follows:

$$\Delta G^0_{Rx} = \sum_{i=1}^{n} \nu_i \cdot \Delta G^0_{fi} \quad (12)$$

where ΔG^0_{fi} is the change in Gibbs free energy of formation of compound i, and ν is the stoichiometric coefficient of compound i in the reaction Rx.

The ΔG^0_{Rx} value at the SOFC operation temperature (T_{SOFC}) and reference temperature (T^*) is calculated by the Van't Hoff equation:

$$\frac{\Delta G^0_{Rx,T_{SOFC}}}{T_{SOFC}} = \frac{\Delta G^0_{Rx}}{T^*} + \int_{T^*}^{T_{SOFC}} -\frac{\Delta H^0_{Rx,T}}{(T_{SOFC})^2}\cdot dT \quad (13)$$

The reversible potentials of the cells ($E_{RevCell1}$ and $E_{RevCell2}$) as a function of the reactant and product concentrations are computed as follows:

$$E_{RevCell} = E^0_{RevCell1}(T_{SOFC}) + \frac{R_g T_{SOFC}}{2Fa}\left[\ln\left(p^*_{H_2,E7\text{-}1}\right) + \frac{1}{2}\ln\left(p^*_{O_2,E9\text{-}2}\right) - \ln\left(p^*_{H_2O,E12\text{-}1}\right)\right] \quad (14)$$

$$E_{RevCell} = E^0_{RevCell2}(T_{SOFC}) + \frac{R_g T_{SOFC}}{2Fa}\left[\ln\left(p^*_{CO,E7\text{-}1}\right) + \frac{1}{2}\ln\left(p^*_{O_2,E9\text{-}2}\right) - \ln\left(p^*_{CO_2,E12\text{-}1}\right)\right] \quad (15)$$

where $E^0_{RevCell1}(T_{SOFC})$ and $E^0_{RevCell2}(T_{SOFC})$ are reversible potentials computed by Eqs. (11)–(13); R_g is the universal gas constant (8.314 J K^{-1} mol^{-1}); $p^*_{H_2,E7\text{-}1}$ and $p^*_{H_2O,E12\text{-}1}$ are the H_2 and H_2O partial pressures at the anode of the first cell, respectively; $p^*_{O_2,E9\text{-}2}$ is the O_2 partial pressure at the cathode of the first cell; analogously, $p^*_{CO,E7\text{-}1}$, $p^*_{CO_2,E12\text{-}1}$ and $p^*_{O_2,E9\text{-}2}$ are the CO and CO_2 partial pressures at the anode, and the O_2 partial pressure at the cathode of the second cell, respectively.

The activation, concentration and ohmic overpotentials are grouped in an unique parameter: $\gamma = 0.2$ V, which is a typical value for SOFC units [2,21].

The H_2 and CO utilization factors at the anode (Fu_{H_2} and Fu_{CO}, respectively) and the O_2 one at the cathode (Fu_{O_2}) are fixed at 0.9 [14].

The power produced by the SOFC unit (Pow_{SOFC}) is computed as follows:

$$\mathrm{Pow_{SOFC}} = (E_{\mathrm{RevCell1}} - \gamma)\cdot I_{\mathrm{Cell1}} + (E_{\mathrm{RevCell2}} - \gamma)\cdot I_{\mathrm{Cell2}} \quad (16)$$

where the current I in each cell is computed by:

$$I_{\mathrm{Cell1}} = \mathrm{Fa}\cdot \mathrm{ne}\cdot \mathrm{Fu_{H_2}}\cdot F_{\mathrm{H_2},C_{7-1}} \quad (17)$$

$$I_{\mathrm{Cell2}} = \mathrm{Fa}\cdot \mathrm{ne}\cdot \mathrm{Fu_{CO}}\cdot F_{\mathrm{CO},C_{7-1}} \quad (18)$$

where $F_{\mathrm{H_2},C_{7-1}}$ and $F_{\mathrm{CO},C_{7-1}}$ are the H_2 and CO inlet flows to the anode of cell Cell1 and Cell2, respectively. For both cells, the number of involved electrons ne is 2.

The heat dissipated by the SOFC unit (Q_{SOFC}) is computed as:

$$Q_{\mathrm{SOFC}} = \mathrm{Hvm}_{C_{11-1}} - \mathrm{Hvm}_{C_{9-2}} + \mathrm{Hvm}_{C_{12-1}} - \mathrm{Hvm}_{C_{6-2}} + \mathrm{Pow_{SOFC}} \quad (19)$$

where $\mathrm{Hvm}_{C_{11-1}}$ and $\mathrm{Hvm}_{C_{9-2}}$ are the outlet and inlet enthalpy values at the cathode, respectively, while $\mathrm{Hvm}_{C_{12-1}}$ and $\mathrm{Hvm}_{C_{6-2}}$ at the anode.

3.6. Combustor

The combustor unit was modeled as the hot utility that provides the energy required for the whole SOFC system. Output gases from the cell anode and cathode and, eventually, an additional extra amount of vaporized fuel are burned in the combustor. When necessary, this extra amount of burned fuel provides the additional heat for satisfying the energy requirements of the whole system.

The combustor exhausted gases are directed to a turbine that powers pumps and two compressors for compressing the air stream needed for combustion and by the electrochemical processes occurring at the SOFC unit. This turbine–compressors–pumps arrangement renders extra power increasing consequently the net global efficiency of the whole system. The turbine can also provide power to the SOFC system. Different configurations are developed in Section 6.

Isentropic behavior is assumed for pumps, compressors and turbine, whose outlet and inlet streams are characterized by their states.

For a given process unit, the transferred and exchanged heat flows are calculated as the difference of the enthalpy values of the stream-states at the unit's outlet and inlet. Fig. 3 identifies the possible heat exchange opportunities for the investigated process.

3.7. Energy integration model

Yee and Grossmann [22] proposed a mixed integer nonlinear programming MINLP model to solve heat exchangers network (HEN) synthesis and design problems, known as the SYNHEAT model. The restrictions and objective function of the SYNHEAT model are included below to introduce in the next subsection the modifications proposed in this paper.

3.7.1. Yee and Grossmann's model

The Yee and Grossmann's model [22] is referred hereafter as the "original model".

Overall energy balance for hot stream i and cold stream j:

$$\left(T_{\mathrm{IN}_i} - T_{\mathrm{OUT}_i}\right)\cdot \dot{m}_i \cdot cp_i = \sum_{k\in \mathrm{ST}}\sum_{j\in \mathrm{CS}} q_{i,j,k} + q_{\mathrm{CU},i} \;\; i\in \mathrm{HS} \quad (20)$$

$$\left(T_{\mathrm{OUT}_j} - T_{\mathrm{IN}_j}\right)\cdot \dot{m}_j \cdot cp_j = \sum_{k\in \mathrm{ST}}\sum_{i\in \mathrm{HS}} q_{i,j,k} + q_{\mathrm{HU},j} \;\; j\in \mathrm{CS} \quad (21)$$

Energy balance for hot stream i and cold stream j in stage k:

$$\left(T_{i,k} - T_{i,k+1}\right)\cdot \dot{m}_i \cdot cp_i = \sum_{j\in \mathrm{CS}} q_{i,j,k} \;\; i\in \mathrm{HS},\; k\in \mathrm{ST} \quad (22)$$

$$\left(T_{j,k} - T_{j,k+1}\right)\cdot \dot{m}_j \cdot cp_j = \sum_{i\in \mathrm{CS}} q_{i,j,k} \;\; j\in \mathrm{CS},\; k\in \mathrm{ST} \quad (23)$$

Inlet temperature assignment for stream i and j:

$$T_{\mathrm{IN}_i} = T_{i,1} \;\; i\in \mathrm{HS} \quad (24)$$

$$T_{\mathrm{IN}_j} = T_{j,k+1} \;\; j\in \mathrm{CS} \quad (25)$$

Temperature feasibility for stream i and j at the interior of stage k:

$$T_{i,k} \geq T_{i,k+1} \;\; i\in \mathrm{HS},\; k\in \mathrm{ST} \quad (26)$$

$$T_{j,k} \geq T_{j,k+1} \;\; j\in \mathrm{CS},\; k\in \mathrm{ST} \quad (27)$$

Temperature feasibility for hot stream i limited by the cold utility temperature:

$$T_{\mathrm{OUT}_i} \leq T_{i,k+1} \;\; i\in \mathrm{HS} \quad (28)$$

Temperature feasibility for cold stream j limited by the hot utility temperature:

$$T_{\mathrm{OUT}_j} \geq T_{j,1} \;\; j\in \mathrm{CS} \quad (29)$$

Energy balance for the cold and hot utilities:

$$\left(T_{i,k+1} - T_{\mathrm{OUT}_i}\right)\cdot \dot{m}_i \cdot cp_i = q_{\mathrm{CU},i} \;\; i\in \mathrm{HS} \quad (30)$$

$$\left(T_{\mathrm{OUT}_j} - T_{j,1}\right)\cdot \dot{m}_j \cdot cp_j = q_{\mathrm{HU},j} \;\; j\in \mathrm{CS} \quad (31)$$

Upper bound constraints for heat exchange:

$$q_{i,j,k} - Q_{\max}\cdot y_{i,j,k} \leq 0 \;\; i\in \mathrm{HS},\; j\in \mathrm{CS},\; k\in \mathrm{ST} \quad (32)$$

$$q_{\mathrm{CU},i} - Q_{\max}\cdot y_{\mathrm{CU},i} \leq 0 \;\; i\in \mathrm{HS} \quad (33)$$

$$q_{\mathrm{HU},j} - Q_{\max}\cdot y_{\mathrm{HU},j} \leq 0 \;\; j\in \mathrm{CS} \quad (34)$$

Minimal allowed temperature difference for heat exchange:

$$\Delta T_{i,j,k} \leq T_{i,k} - T_{j,k} + \Delta T_{i,j}^{\max}\cdot\left(1 - y_{i,j,k}\right) \quad (35)$$

$$\Delta T_{i,j,k+1} \leq T_{i,k+1} - T_{j,k+1} + \Delta T_{i,j}^{\max}\cdot\left(1 - y_{i,j,k}\right) \quad (36)$$

$$\Delta T_{\mathrm{CU},i} \leq T_{i,k+1} - T_{\mathrm{OUT,CU}} + \Delta T_{\mathrm{CU},i}^{\max}\cdot\left(1 - y_{\mathrm{CU},i}\right) \quad (37)$$

$$\Delta T_{\mathrm{HU},j} \leq T_{\mathrm{OUT,HU}} - T_{j,1} + \Delta T_{\mathrm{HU},j}^{\max}\cdot\left(1 - y_{\mathrm{HU},j}\right) \quad (38)$$

Logarithmic mean temperature differences:

$$\mathrm{LMTD}_{i,j,k} - \left[\frac{1}{6}\cdot\left(\Delta T_{i,j,k} + \Delta T_{i,j,k+1}\right) + \frac{2}{3}\cdot\sqrt{\Delta T_{i,j,k}\Delta T_{i,j,k+1}}\right] \leq 0 \quad (39)$$

$$\mathrm{LMTD}_{\mathrm{CU},i} - \left[\frac{1}{6}\cdot\left(\Delta T_{\mathrm{CU},i} + T_{\mathrm{OUT}_i} - T_{\mathrm{IN_{CU}}}\right) + \frac{2}{3}\cdot\sqrt{\Delta T_{\mathrm{CU},i}\cdot\left(T_{\mathrm{OUT}_i} - T_{\mathrm{IN_{CU}}}\right)}\right] \leq 0 \quad (40)$$

$$\mathrm{LMTD}_{\mathrm{HU},j} - \left[\frac{1}{6}\cdot\left(\Delta T_{\mathrm{HU},j} + T_{\mathrm{IN}_{\mathrm{HU}}} - T_{\mathrm{OUT}_j}\right) + \frac{2}{3}\cdot\sqrt{\Delta T_{\mathrm{HU},j}\cdot\left(T_{\mathrm{IN}_{\mathrm{HU}}} - T_{\mathrm{OUT}_j}\right)}\right] \le 0 \quad (41)$$

Heat exchangers area requirements:

$$\mathrm{area}_{i,j,k} - \frac{q_{i,j,k}}{U_{i,j}\cdot\mathrm{LMTD}_{i,j,k}} = 0 \quad (42)$$

$$\mathrm{area}_{\mathrm{CU},i} - \frac{q_{\mathrm{CU},i}}{U_{\mathrm{CU},i}\cdot\mathrm{LMTD}_{\mathrm{CU},i}} = 0 \quad (43)$$

$$\mathrm{area}_{\mathrm{HU},j} - \frac{q_{\mathrm{HU},j}}{U_{\mathrm{HU},j}\cdot\mathrm{LMTD}_{\mathrm{HU},j}} = 0 \quad (44)$$

Total annual cost (objective function):

$$\mathrm{TAC} = \sum_{i\in\mathrm{HS}}\mathrm{CCU}\cdot q_{\mathrm{CU},i} + \sum_{j\in\mathrm{CS}}\mathrm{CHU}\cdot q_{\mathrm{HU},j} + \sum_{i\in\mathrm{HS}}\sum_{j\in\mathrm{CS}}\sum_{k\in\mathrm{ST}}\mathrm{CF}_{i,j}\cdot y_{i,j,k} + \sum_{i\in\mathrm{HS}}\mathrm{CF}_{i,\mathrm{CU}}\cdot y_{\mathrm{CU},i} + \sum_{j\in\mathrm{CS}}\mathrm{CF}_{j,\mathrm{HU}}\cdot y_{\mathrm{HU},j} + \sum_{i\in\mathrm{HS}}\sum_{j\in\mathrm{CS}}\sum_{k\in\mathrm{ST}}\mathrm{CA}_{i,j}\cdot\left(\mathrm{area}_{i,j,k}\right)^{\beta} + \sum_{i\in\mathrm{HS}}\mathrm{CA}_{i,\mathrm{CU}}\cdot\left(\mathrm{area}_{i,\mathrm{CU}}\right)^{\beta_{\mathrm{CU}}} + \sum_{j\in\mathrm{CS}}\mathrm{CA}_{j,\mathrm{HU}}\cdot\left(\mathrm{area}_{j,\mathrm{HU}}\right)^{\beta_{\mathrm{HU}}} \quad (45)$$

3.7.2. *Modifications proposed to the Yee and Grossmann's model*

In this subsection, modifications to the Yee and Grossmann's model are introduced. The resulting mathematical model is referred hereafter as the "modified model".

The reformulation of the original SYNHEAT problem requires modifying some model constraints and adding new ones. More specifically, the product $(\dot{m}\cdot cp\cdot T)$ in the streams energy balances are replaced by the (new) enthalpy variable H. Consequently, Eqs. (24)–(29) related to temperature assignment and feasibility are replaced with the enthalpy assignment constraints. Then, constraints of the original model given by Eqs. (20)–(31) are re-written in the modified model in terms of enthalpy variable as follows:

Overall energy balance for hot stream i and cold stream j:

$$\left(H_{\mathrm{IN}_i} - H_{\mathrm{OUT}_i}\right) = \sum_{k\in\mathrm{ST}}\sum_{j\in\mathrm{CS}} q_{i,j,k} + q_{\mathrm{CU},i} \quad i\in\mathrm{HS} \quad (46)$$

$$\left(H_{\mathrm{OUT}_j} - H_{\mathrm{IN}_j}\right) = \sum_{k\in\mathrm{ST}}\sum_{i\in\mathrm{HS}} q_{i,j,k} + q_{\mathrm{HU},j} \quad j\in\mathrm{CS} \quad (47)$$

Energy balance for hot stream i and cold stream j in stage k:

$$\left(H_{i,k} - H_{i,k+1}\right) = \sum_{j\in\mathrm{CS}} q_{i,j,k} \quad i\in\mathrm{HS},\ k\in\mathrm{ST} \quad (48)$$

$$\left(H_{j,k} - H_{j,k+1}\right) = \sum_{i\in\mathrm{CS}} q_{i,j,k} \quad j\in\mathrm{CS},\ k\in\mathrm{ST} \quad (49)$$

Inlet enthalpy assignment for stream i and j:

$$H_{\mathrm{IN}_j} = H_{j,k+1} \quad j\in\mathrm{CS} \quad (50)$$

$$H_{\mathrm{IN}_i} = H_{i,1} \quad i\in\mathrm{HS} \quad (51)$$

Enthalpy feasibility for stream i and j at the interior of stage k:

$$H_{i,k} \ge H_{i,k+1} \quad i\in\mathrm{HS},\ k\in\mathrm{ST} \quad (52)$$

$$H_{j,k} \ge H_{j,k+1} \quad j\in\mathrm{CS},\ k\in\mathrm{ST} \quad (53)$$

Enthalpy feasibility for hot stream i limited by the cold utility enthalpy:

$$H_{\mathrm{OUT}_i} \le H_{i,k+1} \quad i\in\mathrm{HS} \quad (54)$$

Enthalpy feasibility for cold stream j limited by the hot utility enthalpy:

$$H_{\mathrm{OUT}_j} \ge H_{j,1} \quad j\in\mathrm{CS} \quad (55)$$

Energy balance for the cold and hot utilities

$$\left(H_{i,k+1} - H_{\mathrm{OUT}_i}\right) = q_{\mathrm{CU},i} \quad i\in\mathrm{HS} \quad (56)$$

$$\left(H_{\mathrm{OUT}_j} - H_{j,1}\right) = q_{\mathrm{HU},j} \quad j\in\mathrm{CS} \quad (57)$$

Additional constraints have to be added for relating temperature with enthalpy. More specifically, it is needed to relate Eqs. (46)–(57) with the equations not modified in the original model (Eqs. (32)–(45)). For doing so, constraints given by Eqs. (58) and (59) are added to represent the enthalpy–temperature functionality. It should be noted that this modification allows representing isothermal heat exchanges.

$$T_{i,k} = T_{\mathrm{IN}_i} + \left(T_{\mathrm{OUT}_i} - T_{\mathrm{IN}_i}\right)\cdot\frac{H_{i,k} - H_{\mathrm{IN}_i}}{H_{\mathrm{OUT}_i} - H_{\mathrm{IN}_i}} \quad i\in\mathrm{HS} \quad (58)$$

$$T_{j,k} = T_{\mathrm{IN}_j} + \left(T_{\mathrm{OUT}_j} - T_{\mathrm{IN}_j}\right)\cdot\frac{H_{j,k} - H_{\mathrm{IN}_j}}{H_{\mathrm{OUT}_j} - H_{\mathrm{IN}_j}} \quad j\in\mathrm{CS} \quad (59)$$

3.8. *Process and HEN models integration*

As mentioned earlier, the HEN synthesis problem is traditionally addressed and solved resorting to an *onion skin* scheme, i.e. the heat integration of a given process is performed once the process operation variables were previously optimized [21]. In that case, the stream-states at the process units' inlet and outlet are known values for the heat integration problem. In this paper, the stream-states are decision variables for the optimal synthesis problem, i.e. the operation variables of the process and its integrated HEN are optimized simultaneously.

Then, a new model is derived by coupling the process (SOFC system) model to the HEN model through the enthalpy variable of the stream-states.

The objective function for the optimal synthesis of the process-HEN coupled model is discussed in the following sections.

3.9. *Process streams specifications*

The information source to synthesize the heat exchange network, i.e. the cold and hot streams and their enthalpy and temperature specifications at each state are detailed in Table 3. It should be noted that in the mentioned previous work [23], all entries in Table 3 were known data (fixed values) while in this work they are decision variables to be optimized along with the SOFC system operation variables.

Table 3 – Cold and hot streams to be energetically integrated.

Stream to be integrated	T_{IN}	T_{OUT}	H_{IN}	H_{OUT}
Cold $Q_{1\text{-}1\text{-}2}$	$T_{C_{1,1}}$	$T_{C_{1,2}}$	$H_{C_{1,1}}$	$H_{C_{1,2}}$
Cold $Q_{1\text{-}2\text{-}3}$	$T_{C_{1,2}}$	$T_{C_{1,3}}$	$H_{C_{1,2}}$	$H_{C_{1,3}}$
Cold $Q_{1\text{-}3\text{-}4}$	$T_{C_{1,3}}$	$T_{C_{1,4}}$	$H_{C_{1,3}}$	$H_{C_{1,4}}$
Cold $Q_{2\text{-}1\text{-}2}$	$T_{C_{2,1}}$	$T_{C_{2,2}}$	$H_{C_{2,1}}$	$H_{C_{2,2}}$
Cold $Q_{2\text{-}2\text{-}3}$	$T_{C_{2,2}}$	$T_{C_{2,3}}$	$H_{C_{2,2}}$	$H_{C_{2,3}}$
Cold $Q_{3\text{-}1\text{-}2}$	$T_{C_{3,1}}$	$T_{C_{3,2}}$	$H_{C_{3,1}}$	$H_{C_{3,2}}$
Cold $Q_{4\text{-}1\text{-}2}$	$T_{C_{4,1}}$	$T_{C_{4,2}}$	$H_{C_{4,1}}$	$H_{C_{4,2}}$
Cold Q_{R1}	$T_{C_{5,1}}$	$T_{C_{6,1}}$	$H_{C_{5,1}}$	$H_{C_{6,1}}$
Cold $Q_{6\text{-}1\text{-}2}$	$T_{C_{6,1}}$	$T_{C_{6,2}}$	$H_{C_{6,1}}$	$H_{C_{6,2}}$
Cold $Q_{9\text{-}1\text{-}2}$	$T_{C_{9,1}}$	$T_{C_{9,2}}$	$H_{C_{9,1}}$	$H_{C_{9,2}}$
Cold $Q_{10\text{-}1\text{-}2}$	$T_{C_{10,1}}$	$T_{C_{10,2}}$	$H_{C_{10,1}}$	$H_{C_{10,2}}$
Cold $Q_{13\text{-}1\text{-}2}$	$T_{C_{13,1}}$	$T_{C_{13,2}}$	$H_{C_{13,1}}$	$H_{C_{13,2}}$
Hot Q_{Cell}	$T_{C_{6,3}}$	$T_{C_{12,1}}$	$H_{C_{6,3}}$	$H_{C_{12,1}}$
Hot $Q_{14\text{-}1\text{-}2}$	$T_{C_{14,1}}$	$T_{C_{14,2}}$	$H_{C_{14,1}}$	$H_{C_{14,2}}$
Hot $Q_{14\text{-}3\text{-}4}$	$T_{C_{14,3}}$	$T_{C_{14,4}}$	$H_{C_{14,3}}$	$H_{C_{14,4}}$

3.10. *Overall net process power and efficiency*

The total net power generated by the system (Pow_{System}) is computed as follows:

$$Pow_{System} = Pow_{SOFC} - Pow_{Pumps} - Pow_{Compressors} - \frac{HU}{0.95} - \frac{CU}{25} \quad (60)$$

where Pow_{SOFC}, Pow_{Pumps} and $Pow_{Compressors}$ are the power generated by the SOFC unit, the power required by pumps and compressors, respectively; HU and CU represents the hot and cold utilities, respectively.

The net system efficiency (η^{LHV}_{System}) based on the low heating value (LHV_{Fuel}) is given by:

$$\eta^{LHV}_{System} = \frac{Pow_{System}}{LHV_{Fuel}\left(F_{Fuel,C_{3,2}} + F_{Fuel,C_{5,1}}\right)} \quad (61)$$

where $F_{Fuel,C_{3,2}}$ and $F_{Fuel,C_{5,1}}$ are the fuel molar flow rates fed to the reformer and combustor, respectively.

4. Optimization model statement

The optimization model to synthesize simultaneously the fuel reforming processor for feeding a SOFC unit coupled to a power system, their heat integration, and the number of required heat exchangers can be formulated as a mixed integer nonlinear mathematical programming (MINLP) problem as follows:

$$\begin{aligned} &\text{Max } \eta^{LHV}_{System} \\ &\text{s.t.} \\ &f(x) + g(z) = b \\ &L \le x \le U \\ &z = \{0,1\} \end{aligned} \quad (62)$$

where $f(x)$ and $g(z)$ represents the problem constraints given by Eqs. (1)–(19), (32)–(44), and (46)–(61); x is the vector of continuous variables; and $z(i, j, k)$ is the vector of binary variables, which model the possibilities of heat exchange between process streams i and j in the stage k in the superstructure representation. L and U are the upper and lower bound vectors, respectively; while b represents the vector of independent terms in constraints. By fixing the required system power, all process flows and temperatures as well as the heat exchangers network are synthesized simultaneously based on minimization of energy targets.

5. Resolution methodology and computational aspects

The resulting MINLP model was implemented in *General Algebraic Modeling System GAMS* environment [24], and solved with the *Standard Branch and Bound SBB* code [25].

The resolution of the resulting complex optimization problem was mainly possible by applying a systematic, multistep optimization approach. It consists on the optimization of successive sub problems, which progressively increase the number of involved process streams and states. Each sub problem is first solved to feasibility and then to optimality, posing a different objective function and problem constraints at each solution step. In this approach, the results from a given solution step provide good initial values for solving a larger, more detailed sub problem at the next step, and so on. Following, the approach is described in detail.

It is proposed to solve the optimal synthesis problem (HEN coupled to the fuel processor-SOFC system) through five procedure steps.

5.1. *First solution step*

This step involves the stream-states stream-states $C_{1,1}$ to $C_{1,4}$, $C_{2,1}$ to $C_{2,2}$, $C_{3,1}$ to $C_{3,2}$, $C_{4,1}$ to $C_{4,2}$, $C_{5,1}$, and $C_{6,1}$ to $C_{6,2}$ and includes the reformer model equations and the heat required for the reforming reactions (Q_{R1}), as depicted in Fig. 4. First, the inlet stream-states $C_{1,1}$ and $C_{2,1}$ are initialized with arbitrary values for flows; a molar water/fuel ratio of 9, ambient temperature of 298 K and a system pressure of 3 atm are assumed. In addition, the reformer operation temperature is fixed at 873 K, and the fuel flux directed to the combustor (represented by stream-states $C_{3,1}$ and $C_{3,2}$) is fixed at zero. This sub problem is first solved to obtain a feasible solution, and then the obtained results are used to maximize the objective function for this sub problem ($OF_{Step\ 1}$), which is the ratio between the molar flux of the produced $H_2(F_{H_2,C_{6,1}})$ and the fed fuel ($F_{fuel,C_{2,1}}$):

$$\text{Maximize } OF_{Step\ 1} = \frac{F_{H_2,C_{6,1}}}{F_{fuel,C_{2,1}}} \quad (63)$$

For this optimization problem, the flux of the stream-states $C_{1,1}$ and $C_{2,1}$, the system pressure, and the reformer operating temperature are free variables, i.e. decision variables to be optimized. Lower and upper bounds of 2 and 10 atm, respectively, are assumed for the system pressure. An operating temperature range between 823 and 1073 K is assumed for the reformer. The obtained results are used as initial values for the next solution step.

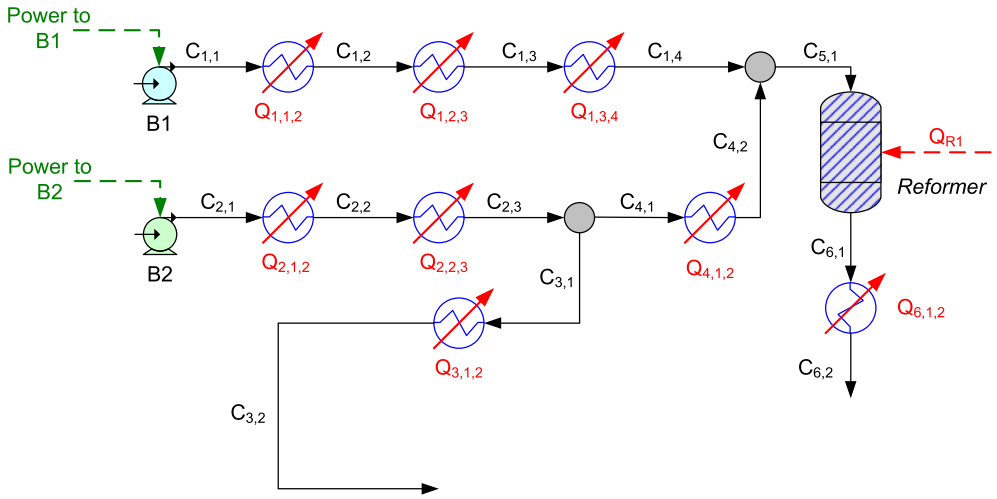

Fig. 4 – First initialization step. Schematic representation of stream-states in the step.

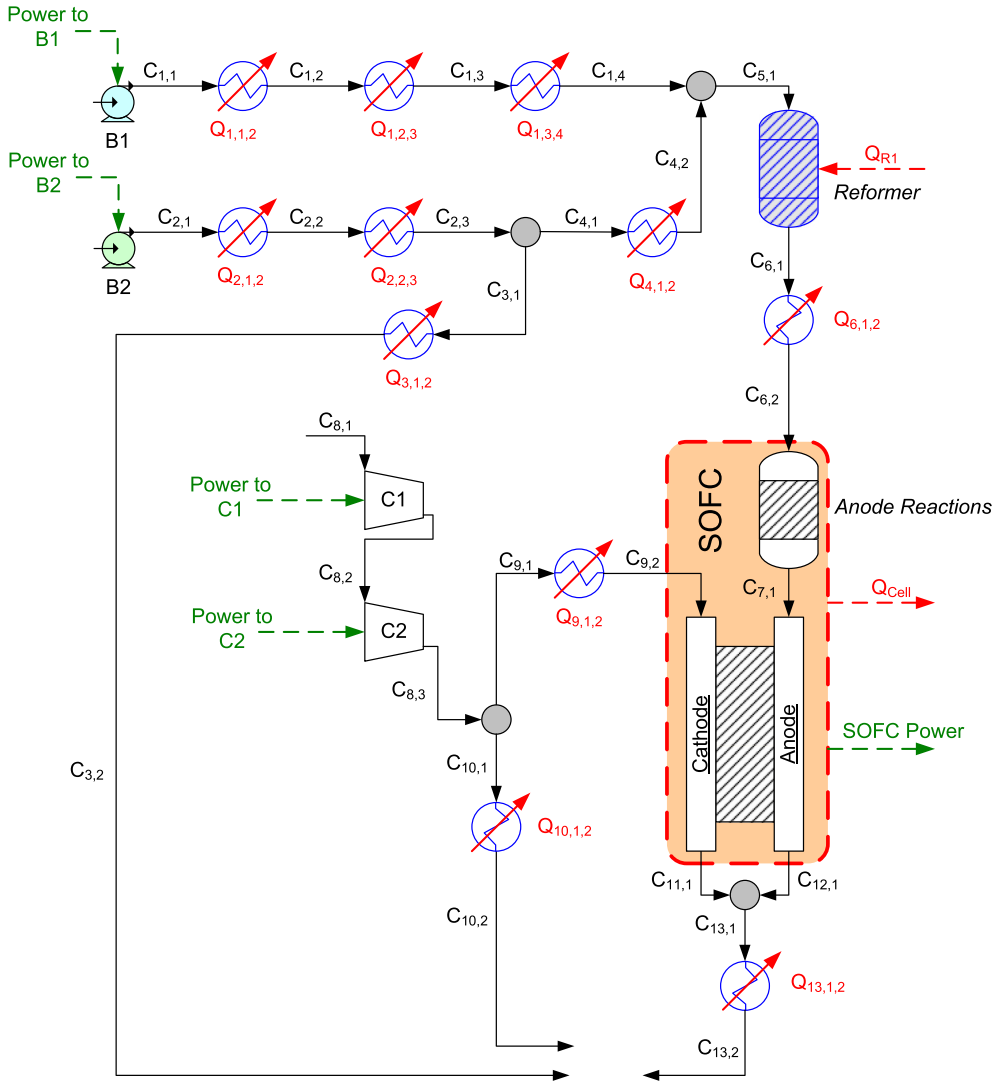

Fig. 5 – Second initialization step. Schematic representation of stream-states in the step.

5.2. Second solution step

As depicted in Fig. 5, this step includes all elements involved in the first solution step along with the stream-sates $C_{7,1}$, $C_{8,1}$–$C_{8,3}$, $C_{9,1}$–$C_{9,2}$, $C_{10,1}$–$C_{10,2}$, $C_{11,1}$, $C_{12,1}$, $C_{13,1}$–$C_{13,2}$, the model equations for the SOFC unit and compressors C1 and C2, the heat dissipated (Q_{Cell}) and the power generated Pow_{SOFC} by the SOFC unit. First, the optimal values obtained in the first solution step are fixed; the remaining model variables (the variables added at this step) are initialized assuming continuity at the involved stream-states. The sub problem is solved to obtain a feasible solution. The obtained results are used afterward to initialize all variables for the optimization problem, except for (i) the air flux of the stream-states $C_{10,1}$–$C_{10,2}$ and the fuel flux of stream-states $C_{3,1}$–$C_{3,2}$, which are fixed to zero; (ii) the temperature of the stream-states $C_{1,1}$, $C_{2,1}$ and $C_{8,1}$, which are fixed at the ambient temperature (298 K); and (iii) the molar water/fuel ratio, which is kept at the value obtained in the first solution step. All other variables are decision variables that maximize the objective function ($OF_{Step\ 2}$) for this sub problem: the power generated by the SOFC unit (Pow_{SOFC}):

$$\text{Maximize } OF_{Step\ 2} = Pow_{SOFC} \tag{64}$$

5.3. Third solution step

This step involves all elements considered at the first and second solution steps along with the stream-states $C_{14,1}$, $C_{14,2}$, $C_{14,3}$, $C_{14,4}$, and the model equations for combustor and turbine T1, as depicted in Fig. 3. Analogously, first, the optimal values obtained in the second solution step are fixed. The flows of the stream-states $C_{3,1}$ and $C_{10,1}$ are initialized with arbitrary values; in this case, the fuel flow fed to the combustor is assumed to be 10% of the fuel flow fed to the reformer, and the air flow fed to the combustor is assumed to 10% of the air flow fed to the SOFC unit. The sub problem is solved to obtain a feasible solution. The obtained values are used afterward as initial values for variables of all states and process units involved in the optimization problem. The objective function ($OF_{Step\ 3}$) for this sub problem is the maximization of the overall net efficiency (η^{LHV}_{System}) of the sub system (with no heat integration):

$$\text{Maximize } OF_{Step\ 3} = \eta^{LHV}_{System} \tag{65}$$

For this optimization sub problem, the hot and cold utilities (HU and CU, respectively) are considered to compute the overall net efficiency η^{LHV}_{System} (Eqs. (60) and (61)). The hot and cold utilities are responsible for satisfying the heating and cooling requirements for changing the states of all involved cold and hot streams, respectively. It should be noted that so far no heat integration between process streams was performed.

5.4. Fourth solution step

In this step, the sub model used in the third solution step (system model without heat integration of process streams) is solved simultaneously with the heat exchange network (HEN) model presented in Section 3.7.2. Here, the inlet and outlet streams temperature and enthalpy values are decision variables to be optimized; i.e. the values of the stream-states and the heat involved in the reaction units without process heat integration are the inlet and outlet values of the hot and cold streams in the HEN model, which are to be optimized. All variables are initialized with optimal values computed in the third step. It should be noted that both sub models share temperature and enthalpy variables. In this step, the optimization problem aims to minimize the requirements of hot and cold utilities in order to favor the heat integration of the process streams over the use of utilities. For that, the overall net system power is fixed at 1 kW. All other model variables are decision variables; some of which may range between lower and upper bounds according to particular specifications or operation constraints. The objective function ($OF_{Step\ 4}$) of the optimization problem for this solution step is:

$$\text{Minimize } OF_{Step\ 4} = HU + CU \tag{66}$$

In case that the computed value for $OF_{Step\ 4}$ is zero at the optimal solution, it means that the whole process does not demand neither hot not cold utilities for generating 1 kW of overall net power. It is said that the system is energetically self-sustainable or self-sufficient.

5.5. Fifth (last) solution step

In this step, the heat exchange network HEN model is coupled to the sub system model used in the previous step. All variables are initialized with the optimal values computed in the forth solution step. The generated overall net power is kept fixed at 1 kW. The hot and cold utilities (HU and CU, respectively) are fixed at zero to guarantee the self-sustainable operation of the integrated process. As in the third solution step, the objective function ($OF_{Step\ 5}$) to be maximized is the overall net efficiency:

$$\text{Maximize } OF_{Step\ 5} = \eta^{LHV}_{System} \tag{67}$$

Although the optimization problems solved in the third and fifth steps maximize the same objective function (the overall net system efficiency), the difference relies in that the heat exchangers network HEN is obtained in the fifth step along with the operation conditions of the entire, integrated process. Whereas in the third solution step the heating and cooling requirements are provided exclusively by auxiliary services with no heat integration of the process streams.

6. Results

The overall net power generated by the SOFC system is fixed at 1 kW for all analyzed cases.

First, an optimization model for addressing simultaneously the determination of the process operation conditions and the synthesis of the coupled heat exchangers network was solved using ethanol as fuel, which has a low heating value LHV of 1235 kJ mol^{-1}. Afterward, the same problem was solved using glycerin, whose LHV is 1477 kJ mol^{-1}.

Table 4 – Optimal values of process operating variables using ethanol for scenarios (a) and (b).

Scenario		(a)									(b)								
Stream	State (IN/OUT)	T (K)	Molar flow per kW generated (mol h^{-1}/$kW_{generated}$)							Heat flow per kW generated ($kW/kW_{generated}$)	T (K)	Molar flow per kW generated (mol h^{-1}/$kW_{generated}$)							Heat flow per kW generated ($kW/kW_{generated}$)
			Ethanol	H_2O	H_2	CH_4	CO	CO_2	O_2	N_2			Ethanol	H_2O	H_2	CH_4	CO	CO_2	O_2	N_2	
Cold $Q_{1,1,2}$	C_{1-1}	298.00		15.56							0.03	298.00		12.609							0.03
	C_{1-2}	393.81		15.56								393.81		12.609							
Cold $Q_{1,2,3}$	C_{1-2}	393.81		15.56							0.17	393.81		12.609							0.14
	C_{1-3}	393.81		15.56								393.81		12.609							
Cold $Q_{1,3,4}$	C_{1-3}	393.81		15.56							0.06	393.81		12.609							0.05
	C_{1-4}	779.05		15.56								783.77		12.609							
Cold $Q_{2,1,2}$	C_{2-1}	298.00	4.85								0.01	298.00	4.203								0.01
	C_{2-2}	369.95	4.85									369.95	4.203								
Cold $Q_{2,2,3}$	C_{2-2}	369.95	4.85								0.05	369.95	4.203								0.04
	C_{2-3}	369.95	4.85									369.95	4.203								
Cold $Q_{3,1,2}$	C_{3-1}										0.00	369.95									0.00
	C_{3-2}											369.95									
Cold $Q_{4,1,2}$	C_{4-1}	369.95	4.85								0.06	369.95	4.203								0.05
	C_{4-2}	779.05	4.85									783.77	4.203								
Cold Q_{R1}	C_{5-1}	779.05	4.85	15.56							0.00	783.77	4.203	12.609							0.00
	C_{6-1}	779.05		12.23	7.15	5.36	0.48	3.85				783.77		9.772	6.129	4.659	0.455	3.292			
Cold $Q_{6,1,2}$	C_{6-1}	779.05		12.23	7.15	5.36	0.48	3.85			0.11	783.77		9.772	6.129	4.659	0.455	3.292			0.09
	C_{6-2}	1073.00		12.23	7.15	5.36	0.48	3.85				1073.00		9.772	6.129	4.659	0.455	3.292			
Cold $Q_{9,1,2}$	C_{9-1}	363.27							14.28	53.73	0.42	363.27							12.347	46.447	0.36
	C_{9-2}	1073.00							14.28	53.73		1073.00							12.347	46.447	
Cold $Q_{10,1,2}$	C_{10-1}	363.26							3.97	14.93	0.00	363.27							0.262	0.987	0.00
	C_{10-2}	363.26							3.97	14.93		363.27							0.262	0.987	
Cold $Q_{13,1,2}$	C_{13-1}	1073.00		27.68	2.17	0.13	0.69	8.88	1.43	53.73	0.00	1073.00		23.097	1.859	0.131	0.611	7.664	1.235	46.447	0.00
	C_{13-2}	1073.00		27.68	2.17	0.13	0.69	8.88	1.43	53.73		1073.00		23.097	1.859	0.131	0.611	7.664	1.235	46.447	
Hot Q_{Cell}	C_{6-2}	1073.00		12.23	7.15	5.36	0.48	3.85			0.49	1073.00		9.772	6.129	4.659	0.455	3.292			0.42
	C_{12-1}	1073.00		27.68	2.17	0.13	0.69	8.88				1073.00		23.097	1.859	0.131	0.611	7.664			
Hot $Q_{14,1,2}$	C_{14-1}	1170.70		30.11				9.70	3.71	68.66	0.42	1297.08		25.218				8.406		47.434	0.00
	C_{14-2}	802.83		30.11				9.70	3.71	68.66		1297.08		25.218				8.406		47.434	
Hot $Q_{14,3,4}$	C_{14-3}	727.12		30.11				9.70	3.71	68.66	0.00	1078.00		25.218				8.406		47.434	0.35
	C_{14-4}	727.12		30.11				9.70	3.71	68.66		649.82		25.218				8.406		47.434	
Anode reactions	C_{6-2}	1073.00		12.23	7.15	5.36	0.48	3.85			–	1073.00		9.772	6.129	4.659	0.455	3.292			–
	C_{7-1}	1073.00		8.17	21.68	0.13	6.88	2.68				1073.00		6.371	18.585	0.131	6.108	2.167			

Table 5 – Optimal values of process operating variables using glycerin for scenarios (a) and (b).

Scenario		(a)									(b)								
Stream	State (IN/OUT)	T (K)	Molar flow per kW generated (mol $h^{-1}/kW_{generated}$)							Heat flow per kW generated ($kW/kW_{generated}$)	T (K)	Molar flow per kW generated (mol $h^{-1}/kW_{generated}$)							Heat flow per kW generated ($kW/kW_{generated}$)
			Glycerin	H_2O	H_2	CH_4	CO	CO_2	O_2	N_2			Glycerin	H_2O	H_2	CH_4	CO	CO_2	O_2	N_2	
Cold $Q_{1,1,2}$	C_{1-1}	298.00		12.48							0.03	298.00		10.918							0.02
	C_{1-2}	394.63		12.48								393.81		10.918							
Cold $Q_{1,2,3}$	C_{1-2}	394.63		12.48							0.14	393.81		10.918							0.12
	C_{1-3}	394.63		12.48								393.81		10.918							
Cold $Q_{1,3,4}$	C_{1-3}	394.63		12.48							0.06	393.81		10.918							0.05
	C_{1-4}	851.80		12.48								850.47		10.918							
Cold $Q_{2,1,2}$	C_{2-1}	298.00	4.16								0.10	298.00	3.639								0.09
	C_{2-2}	588.31	4.16									587.29	3.639								
Cold $Q_{2,2,3}$	C_{2-2}	588.31	4.16								0.07	587.29	3.639								0.06
	C_{2-3}	588.31	4.16									587.29	3.639								
Cold $Q_{3,1,2}$	C_{3-1}																				0.00
	C_{3-2}																				
Cold $Q_{4,1,2}$	C_{4-1}	588.31	4.16								0.06	587.29	3.639								0.05
	C_{4-2}	851.80	4.16									850.47	3.639								
Cold Q_{R1}	C_{5-1}	851.80	4.16	12.48							0.00	850.47	3.639	10.918							0.00
	C_{6-1}	1073.00		10.34	10.66	4.06	2.21	6.21				850.47		9.032	9.338	3.552	1.927	5.438			
Cold $Q_{6,1,2}$	C_{6-1}	1073.00		10.34	10.66	4.06	2.21	6.21			0.09	850.47		9.032	9.338	3.552	1.927	5.438			0.08
	C_{6-2}	1073.00		10.34	10.66	4.06	2.21	6.21				1073.00		9.032	9.338	3.552	1.927	5.438			
Cold $Q_{9,1,2}$	C_{9-1}	365.94							14.33	53.91	0.42	363.27							12.544	47.189	0.37
	C_{9-2}	1073.00							14.33	53.91		363.27							12.544	41.189	
Cold $Q_{10,1,2}$	C_{10-1}	365.94							0.23	0.87	0.00	363.27							0.193	0.727	0.00
	C_{10-2}	365.94							0.23	0.87		363.27							0.193	0.727	
Cold $Q_{13,1,2}$	C_{13-1}	1073.00		26.88	2.01	0.12	0.85	11.51	1.43	53.91	0.00	1073.00		23.519	1.762	0.097	0.746	10.074	1.254	47.189	0.00
	C_{13-2}	1073.00		26.88	2.01	0.12	0.85	11.51	1.43	53.91		1073.00		23.519	1.762	0.097	0.746	10.074	1.254	47.189	
Hot Q_{Cell}	C_{6-2}	1073.00		10.34	10.66	4.06	2.21	6.21			0.58	1073.00		9.032	9.338	3.552	1.927	5.438			0.51
	C_{12-1}	1073.00		26.88	2.01	0.12	0.85	11.51				1073.00		23.519	1.762	0.097	0.746	10.074			
Hot $Q_{14,1,2}$	C_{14-1}	1285.00		29.12				12.48		54.77	0.38	1284.30		25.474				10.918		47.916	0.00
	C_{14-2}	916.97		29.12				12.48		54.77		1284.30		25.474				10.918		47.916	
Hot $Q_{14,3,4}$	C_{14-3}	837.28		29.12				12.48		54.77	0.00	1078.03		25.474				10.918		47.916	0.34
	C_{14-4}	837.28		29.12				12.48		54.77		689.51		25.474				10.918		47.916	
Anode reactions	C_{6-2}	1073.00		10.34	10.66	4.06	2.21	6.21			–	1073.00		9.032	9.338	3.552	1.927	5.438			–
	C_{7-1}	1073.00		8.76	20.13	0.12	8.53	3.84				1073.00		7.658	17.623	0.097	7.464	3.356			

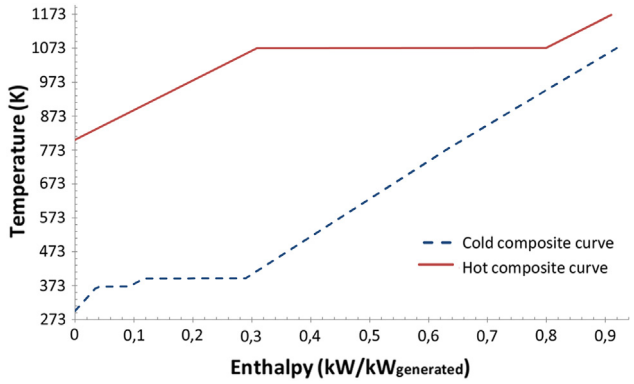

Fig. 6 – Composite curves of scenario (a) using ethanol.

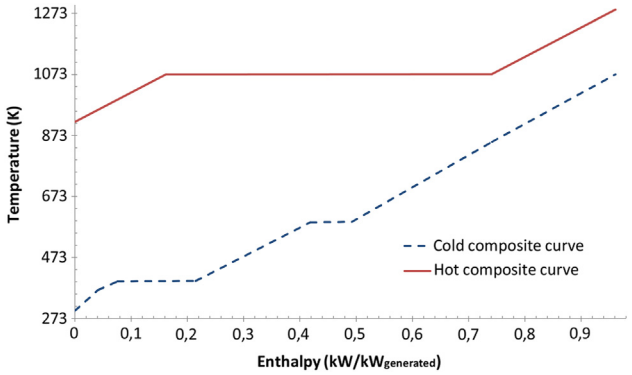

Fig. 8 – Composite curves of scenario (a) using glycerin.

Regardless the fuel used, the following process input data reported in literature as practical operation values are assumed for the examined process. The operation temperature of the SOFC unit is assumed to range between 1073 and 1273 K, and the reformer between 673 and 873 K. The lower and upper bounds for the water/fuel molar ratio are fixed at 3 and 13, respectively. The variation range of the total system pressure is from 2 to 10 atm. The inlet temperatures of the fuel, water and air streams fed to the SOFC system are fixed at 298 K. The temperatures of the other states can vary between 273 and 2000 K. All state values are expressed per 1 kW of net power generated.

Two different scenarios are optimized depending on the operation specifications assumed for the expander turbine T1:

(a) Expander turbine T1 is driven by exhaust gases from the combustor and can only supply power to pumps (B1 and B2) and compressors (C1 and C2). The mechanical energy of the turbine is delivered to the compressors by mechanical devices. This scenario considers turbo-compressor and turbo-pump units.
(b) Besides to power the referred pumps and compressors as in scenario (a), T1 can also contribute to the total net power of the system; i.e. in addition to the mechanical devices used in compressors, electronic devices are required to convert the mechanical energy of the turbine into electric energy (turbo-generator), which is added to the amount produced by the SOFC.

Tables 4 and 5 include the optimal operation values of the SOFC system for the examined scenarios using ethanol and glycerin, respectively. The composite curves of the heat exchangers network for scenario (a) and scenario (b) using ethanol are represented in Figs. 6 and 7, respectively, and in Figs. 8 and 9 using glycerin. Analogously, the resulting optimal heat exchangers networks using ethanol are represented in Figs. 10 and 11 for scenarios (a) and (b), respectively, and in Figs. 12 and 13 using glycerin.

Finally, a comparison of the obtained optimal values of the main process variables for the four cases analyzed is presented in Table 6. From a thermodynamic point of view, these values correspond to the maximum net efficiency of the SOFC system.

7. Discussions

The computed optimal water/ethanol and water/glycerin ratios for all scenarios are close to the lower bound (Table 6), which was set at 3. From an energetic point of view, it is preferable a low water fraction in the SOFC system since water must be vaporized at around 800 K with a large vaporization latent heat, requiring thus a significant energy amount (see

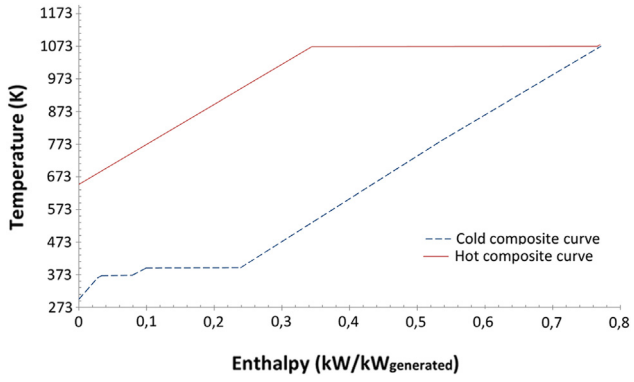

Fig. 7 – Composite curves of scenario (b) using ethanol.

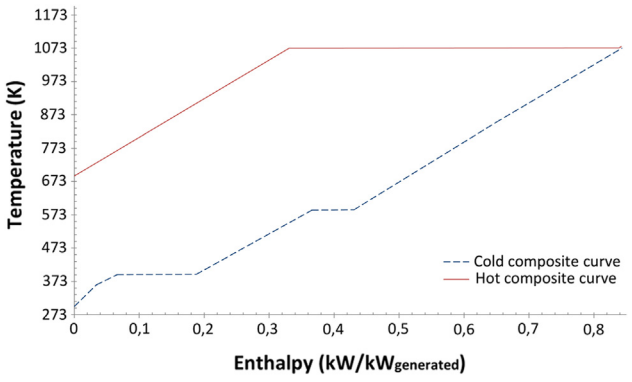

Fig. 9 – Composite curves of scenario (b) using glycerin.

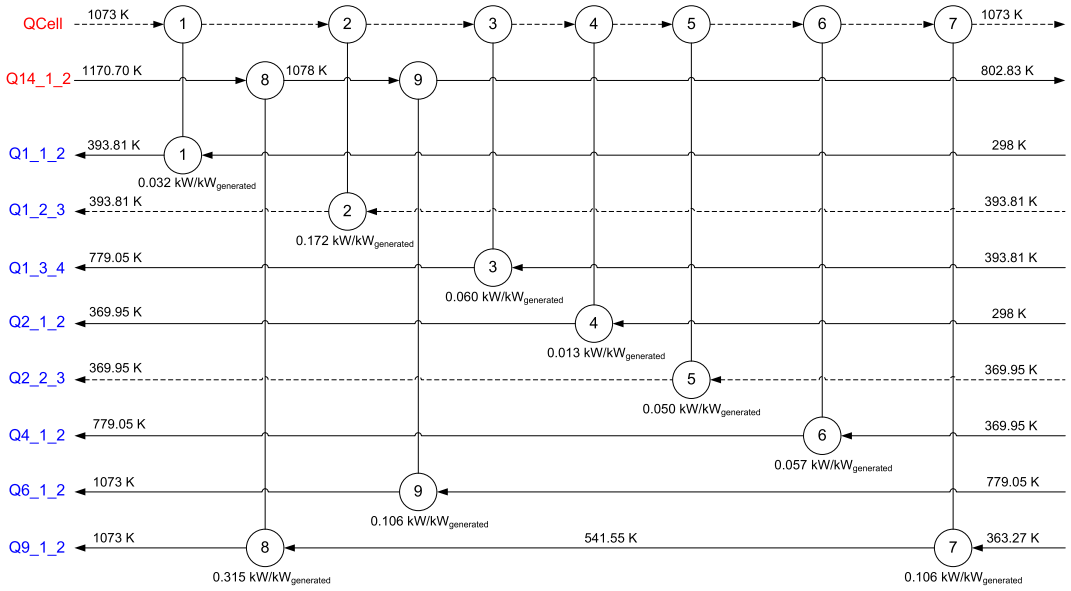

Fig. 10 – Heat exchangers network of scenario (a) using ethanol as fuel.

Figs. 10–13). The resulting optimal low water/fuel molar ratios can also be explained by the fact that water is a product in the electrochemical reaction at the anode; i.e. water excess shifts the reaction to produce low energy levels in the SOFC. This effect can be evaluated through Eq. (14), which represents the reversible potential.

Note that in all scenarios the heat exchanged at the reformer is zero (Q_{R1}). This suggests that only alcohol decomposition reactions occur at the reformer.

For all examined scenarios, the SOFC system operates optimally without burning extra fuel at the combustor (see streams $C_{3,1}$ and $C_{3,2}$ in Tables 4 and 5). This behavior can be related to the auto-thermal reforming, but in this case, the reforming reactions and oxidation occur separately.

Regardless of the used fuel and the examined scenario, the largest energy demand is for heating the inlet air to the cathode (Figs. 10–13), what should be considered at the design phase.

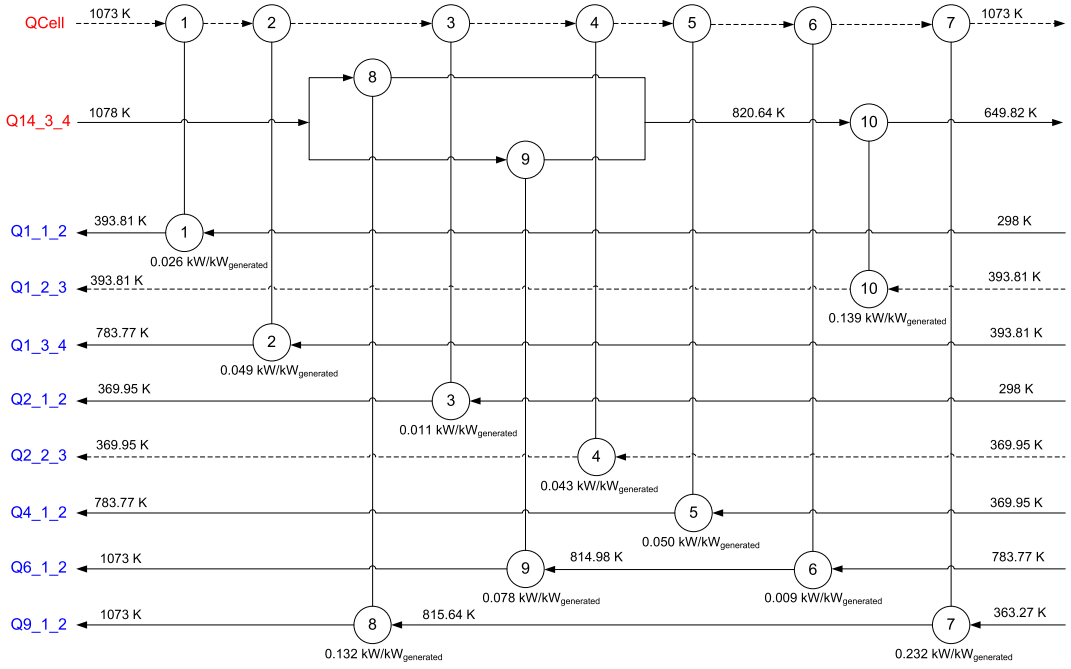

Fig. 11 – Heat exchangers network of scenario (b) using ethanol as fuel.

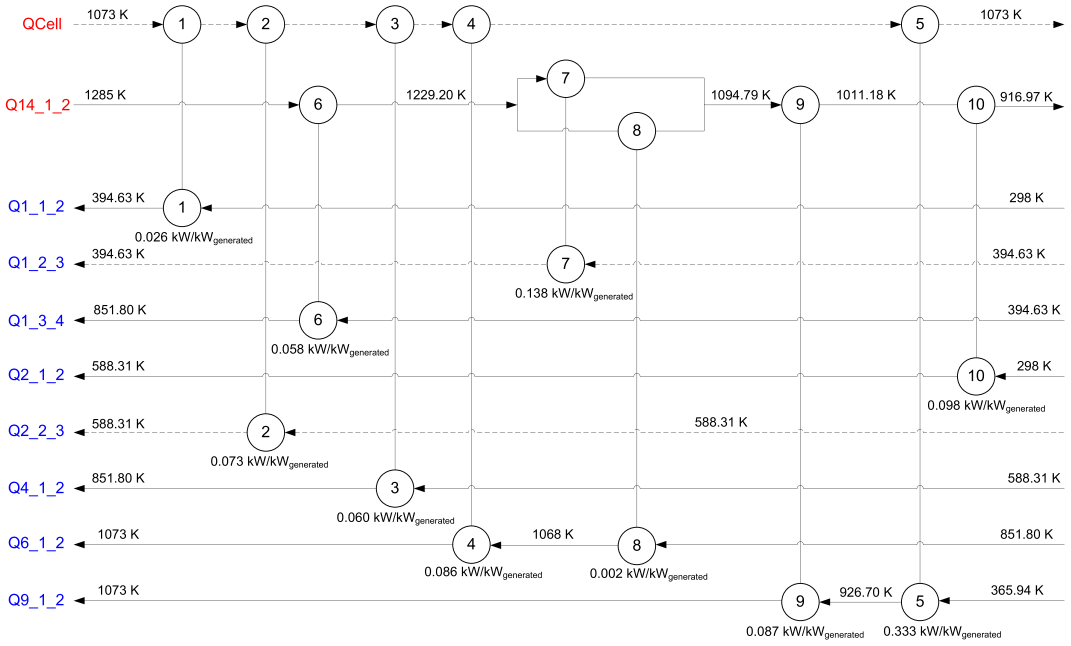

Fig. 12 – Heat exchangers network of scenario (a) using glycerin as fuel.

It should be noted from Figs. 6–9 the high temperature values of the hot composite curve for all scenarios. This is because of the high temperature level at which the SOFC operates, and by the fact that the optimization seeks the best operation conditions of the turbine. The system is energetically self-sufficient, requiring no auxiliary services. The efficiency can be improved by coupling another power system to the SOFC system, i.e. using the high temperature level of the exhaust gases of the SOFC system in a steam power cycle.

The optimal operation pressure of the SOFC system tends to the lower bound fixed in all scenarios (2 atm). Probably this behavior is related with a tradeoff among the energy consumed by compressors, the energy produced by the turbine, and the latent vaporization heat of the water. Power

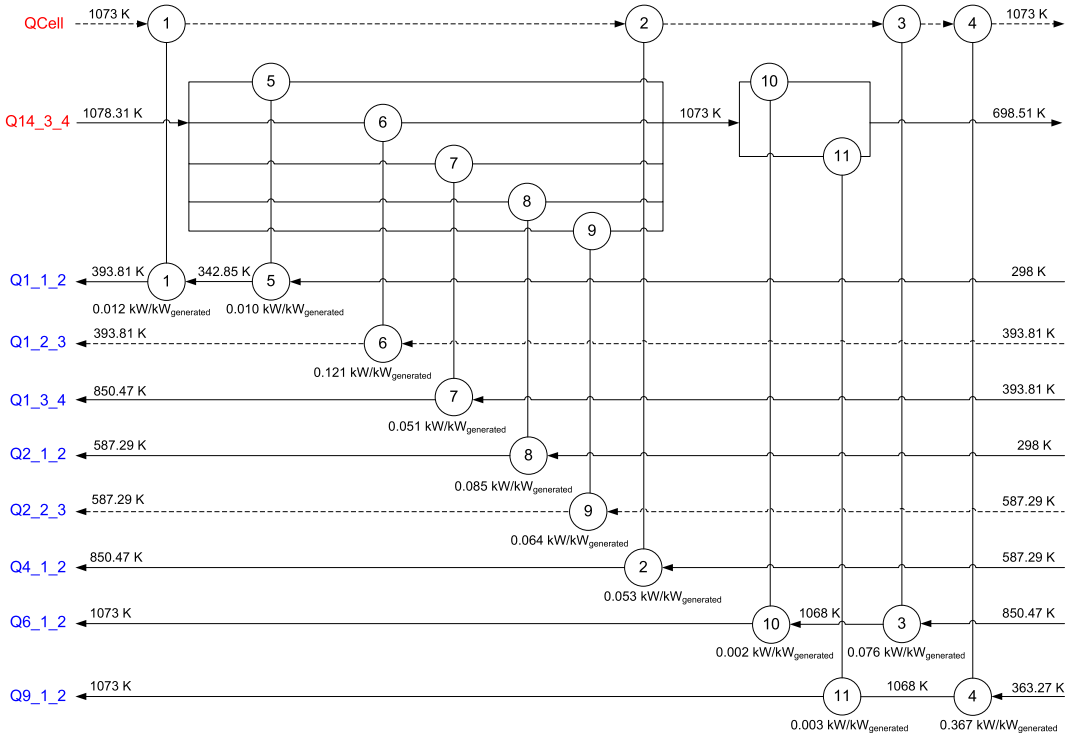

Fig. 13 – Heat exchangers network of scenario (b) using glycerin as fuel.

Table 6 – Comparative chart of the main process variables depending on the fuel used and scenario.

Scenario	Ethanol		Glycerin	
	(a)	(b)	(a)	(b)
Net efficiency based on LHV	60.14	69.35	58.59	66.97
SOFC system pressure (atm)	2.00	2.00	2.05	2.00
Water/fuel molar ratio	3.211	3.00	3.00	3.00
Water pump power per kW generated ($kW/kW_{generated}$)	0.011	0.009	0.009	0.007
Fuel pump power per kW generated ($kW/kW_{generated}$)	0.011	0.009	0.019	0.016
Power consumption of compressors per kW generated ($kW/kW_{generated}$)	0.061	0.042	0.051	0.042
Power supplied by the turbine per kW generated ($kW/kW_{generated}$)	0.083	0.193	0.079	0.191
Power supplied by the SOFC per kW generated ($kW/kW_{generated}$)	1.000	0.867	1.000	0.875
SOFC voltage (V)	0.725	0.727	0.722	0.722
Reformer temperature (K)	779.05	783.77	851.80	850.47
SOFC temperature (K)	1073.00	1073.00	1073.00	1073.00
Output temperature of the SOFC system (K)	727.12	649.82	837.28	689.51
Output pressure of the SOFC system (atm)	1.387	1.000	1.467	1.046

generated by the turbine is also related with the outlet combustor temperature.

The computed total energy exchanged in the heat exchangers network depends on the used fuel. For scenario (a), the energy level in composite curves for glycerin is higher than ethanol, as observed by comparing Figs. 6 and 8. The same observation is made for scenario (b) by comparing Figs. 7 and 9. This is, at the design phase, SOFC systems fed with glycerin will be bigger in size than the systems operated with ethanol.

This new methodology allows optimizing simultaneously the operation variables of the process and its energy and mass integration. Traditional methodologies perform separately these optimizations: first, the operation variables are optimized, and then, mass and energy integration of the process streams is performed.

A sensitivity analysis to the optimization variables should be performed to evaluate the effects of the different design and operation variables to the optimal solution obtained for each case. Those results may provide recommended operation ranges of the main process variables and parameters to obtain good alternative suboptimal solutions of practical interest. This aspect will be addressed in a further paper.

8. Conclusions

A new methodology for optimizing simultaneously process operation and heat exchangers network synthesis has been presented. A systematic model initialization procedure has been developed.

The proposed approach is of general application in process industry. In this paper, this methodology has been applied to optimize solid oxide fuel cell SOFC systems under different scenarios. As the net global energy efficiency of this type of systems is actually low, efforts has to be focused on elucidating the main energy trade-offs to make fuel cell systems more attractive than (conventional and nonconventional) competitive, alternative energy systems.

Ethanol and glycerin were studied as fuels fed to the SOFC system as they constitute two renewable and sustainable sources of energy. In addition, two different operation specifications of an expander turbine were considered.

The best global net efficiency values are obtained for scenario (b). The SOFC system fed with ethanol and glycerin as fuels reaches a net global efficiency of 69.35% and 66.97%, respectively. In both cases the optimal operation pressure is 2 atm. The computed SOFC operation temperature for all scenarios is 1073 K (lower bound). The optimal reformer temperature in scenario (b) varies depending on the fuel used: 783.77 K for ethanol and 850.47 K for glycerin. A similar behavior is obtained in scenario (a): 779.05 K for ethanol and 851.80 K for glycerin.

The computed optimal water/fuel molar ratio value is around 3 for all studied cases. Depending on the cases, the optimal outlet SOFC system temperature ranges between 649 and 838 K. Then, a steam power system can be coupled to the SOFC system to increase the net global system efficiency. This issue will be addressed in a future work.

Acknowledgment

The authors acknowledge the financial support from CONICET (Consejo Nacional de Investigaciones Científicas y Técnicas) and ANCYPT (Agencia Nacional de Promoción Científica y Técnica) from Argentina.

Nomenclature

$C_{r,j}$	stream r at state j
E	electric potential, V
E^0	electric potential at standard conditions, V
$F_{i,s}$	molar flow of component i at stream s, mol h^{-1}
Fa	Faraday constant, 96,487 C mol^{-1}
Fu_i	utilization factor of component i
I	electric current at cell, A
$H_{i,s}$	enthalpy of the component i at stream s, kJ mol^{-1}
Hl_l	enthalpy of the liquid stream l, kJ mol^{-1}
$Hv_{i,j}$	enthalpy of component i at state j, kJ mol^{-1}
Hvm_s	enthalpy flow in stream s, kW
Keq_{Rx}	equilibrium constant in reaction Rx

LHV	low heating value, kW h mol^{-1}
ne	number of electrons transferred in the reaction
P^*	inlet partial pressure at cell, atm
P_{total}	total pressure in the system, atm
P_i	partial pressure of component *i*, atm
Pow	power, kW
$Q_{p,m,n}$	heat transferred from stream *p* to change its state *m* to *n*, kW
R_g	universal gas constant 8.314 J K^{-1} mol^{-1}
SOFC	solid oxide fuel cell
T_j	temperature of state *j*, K
T_{ref}	reference temperature, K
Ts	temperature of phase change, K
HU	hot utility, kW
CU	cold utility, kW
z	binary variable representing existence of a heat exchanger

Greek letters

α	Antoine coefficient
β	correlation coefficient
δ	correlation coefficient
ϕ	correlation coefficient
γ	SOFC overpotential
ν_i	stoichiometric coefficient of compound *i* in the reaction
$\eta_{Sistema}$	system efficiency
$\Delta H_{form,i}$	enthalpy of formation of compound *i*, J mol^{-1}
ΔH_{Liq_l}	energy necessary to change the liquid stream *l* from liquid state temperature to the temperature Ts, kJ mol^{-1}
ΔH_{Vap_l}	latent vaporization heat of stream *l*, kJ mol^{-1}

Subscript

a	anode
c	cathode
Cell1	cell for H_2 oxidation
Cell2	cell for CO oxidation
i	gaseous component *i*
l	liquid component *l*
j	state
r	stream
s	stream
RevCell1	reversible of Cell1
RevCell2	reversible of Cell2
Rx	reaction
SOFC	solid oxide fuel cell

REFERENCES

[1] Janardhanan VM, Deutschmann O. Modeling of solid-oxide fuel cells. Zeitschrift Für Physikalische Chemie 2007;221(4):443–78.

[2] Ni M, Leung MKH, Leung DYC. Parametric study of solid oxide fuel cell performance. Energy Conversion and Management 2007;48(5):1525–35.

[3] Yakabe H, Ogiwara T, Hishinuma M, Yasuda I. 3-D model calculation for planar SOFC. Journal of Power Sources 2001;102(1–2):144–54.

[4] Achenbach E. Three-dimensional and time-dependent simulation of a planar solid oxide fuel cell stack. Journal of Power Sources 1994;49(1–3):333–48.

[5] Bhattacharyya D, Rengaswamy R, Finnerty C. Dynamic modeling and validation studies of a tubular solid oxide fuel cell. Chemical Engineering Science 2009;64(9):2158–72.

[6] Mollayi Barzi Y, Ghassemi M, Hamedi MH. A 2D transient numerical model combining heat/mass transport effects in a tubular solid oxide fuel cell. Journal of Power Sources 2009;192(1):200–7.

[7] Cimenti M, Hill JM. Thermodynamic analysis of solid oxide fuel cells operated with methanol and ethanol under direct utilization, steam reforming, dry reforming or partial oxidation conditions. Journal of Power Sources 2009;186(2):377–84.

[8] Bove R, Lunghi P, Sammes NM. SOFC mathematic model for systems simulations. Part one: from a micro-detailed to macro-black-box model. International Journal of Hydrogen Energy 2005;30(2):181–7.

[9] Burbank W, Witmer DD, Holcomb F. Model of a novel pressurized solid oxide fuel cell gas turbine hybrid engine. Journal of Power Sources 2009;193(2):656–64.

[10] Cocco D, Tola V. Use of alternative hydrogen energy carriers in SOFC–MGT hybrid power plants. Energy Conversion and Management 2009;50(4):1040–8.

[11] Costamagna P, Magistri L, Massardo AF. Design and part-load performance of a hybrid system based on a solid oxide fuel cell reactor and a micro gas turbine. Journal of Power Sources 2001;96(2):352–68.

[12] Petruzzi L, Cocchi S, Fineschi F. A global thermo-electrochemical model for SOFC systems design and engineering. Journal of Power Sources 2003;118(1–2):96–107.

[13] Yi Y, Rao AD, Brouwer J, Samuelsen GS. Analysis and optimization of a solid oxide fuel cell and intercooled gas turbine (SOFC–ICGT) hybrid cycle. Journal of Power Sources 2004;132(1–2):77–85.

[14] Arteaga-Perez LE, Casas Y, Peralta LM, Kafarov V, Dewulf J, Giunta P. An auto-sustainable solid oxide fuel cell system fueled by bio-ethanol: process simulation and heat exchanger network synthesis. Chemical Engineering Journal 2009;150(1):242–51.

[15] Palazzi F, Autissier N, Marechal FMA, Favrat D. A methodology for thermo-economic modeling and optimization of solid oxide fuel cell systems. Applied Thermal Engineering 2007;27(16):2703–12.

[16] Autissier N, Palazzi F, Marechal F, Van Herle J, Favrat D. Thermo-economic optimization of a solid oxide fuel cell, gas turbine hybrid system. Journal of Fuel Cell Science and Technology 2007;4(2):123–9.

[17] Santin M, Traverso A, Magistri L. Liquid fuel utilization in SOFC hybrid systems. Applied Energy 2009;86(10):2204–12.

[18] Francesconi JA, Mussati MC, Mato RO, Aguirre PA. Analysis of the energy efficiency of an integrated ethanol processor for PEM fuel cell systems. Journal of Power Sources 2007;167(1):151–61.

[19] Hirai T, Ikenaga N, Miyake T, Suzuki T. Production of hydrogen by steam reforming of glycerin on ruthenium catalyst. Energy & Fuels 2005;19(4):1761–2.

[20] Godat J, Marechal F. Optimization of a fuel cell system using process integration techniques. Journal of Power Sources 2003;118(1–2):411–23.

[21] Ni M, Leung DYC, Leung MKH. Electrochemical modeling and parametric study of methane fed solid oxide fuel cells. Energy Conversion and Management 2009;50(2):268–78.

[22] Yee TF, Grossmann IE. Simultaneous optimization models for heat integration – II. Heat exchanger network synthesis. Computers & Chemical Engineering 1990;14(10):1165–84.

[23] Oliva DG, Francesconi JA, Mussati MC, Aguirre PA. Modeling, synthesis and optimization of heat exchanger networks. Application to fuel processing systems for PEM fuel cells. International Journal of Hydrogen Energy 2011;36(15):9098–114.

[24] Brooke A. GAMS language guide release 2.25, vol. 92. GAMS Development Corporation; 1997.

[25] Linderoth JT, Savelsbergh MWP. A computational study of search strategies for mixed integer programming. INFORMS Journal on Computing 1999;11(2):173–87.